Near critical states of random Dirac fermions

Y. Morita and Y. Hatsugai

Department of Applied Physics, University of Tokyo, 7-3-1 Hongo Bunkyo-ku, Tokyo 113, Japan

(May 2)

Abstract

Random Dirac fermions in a two-dimensional space are studied numerically. We realize them on a square lattice using the π-flux model with random hopping. The system preserves two symmetries, the time-reversal symmetry and the symmetry denoted by $\{\mathcal{H}, \gamma\} = 0$ with a 4×4 matrix γ in an effective field theory. Although it belongs to the orthogonal ensemble, the zero-energy states do not localize and become *critical*. The density of states vanishes at zero energy as $\sim E^{\alpha}$ and the exponent α changes with strength of the randomness, which implies the existence of the critical line. Rapid growth of the localization length near zero energy is suggested and the eigenstates near zero energy exhibit anomalous behaviour which can be interpreted as a *critical slowing down* in the available finite-size system. The level-spacing distributions close to zero energy deviate from both the Wigner surmise and the Poissonian, and exhibit critical behaviour which reflects the existence of critical states at zero energy.

Dirac fermions often appear in condensed matter physics, for example, a transition between different quantum Hall states [1–3], two-dimensional graphite sheets [4], a mean-field theory of the t-J model ('π-flux state') [5] and d-wave superconductors [6]. It is then natural to investigate what happens when disorder is included. Random Dirac fermions in a two-dimensional space were investigated by several groups [6–12]. Possible appearance of non-localized states, critical states, in random Dirac fermions was pointed out in [7]. Recently, this disordered critical state was realized in a lattice model, where it was crucial to preserve a symmetry denoted by $\{\mathcal{H}, \gamma\} = 0$ with a 4×4 matrix γ in an effective field theory [8] (see below).

In this paper, we study the random Dirac fermions numerically beyond the zero modes. In order to realize the massless Dirac fermions on a two-dimensional lattice, we use a tight-binding model on a square lattice with half a flux quantum ('π flux') per plaquette, which is described by the Hamiltonian

$$H_{pure} = \sum_{<i,j>} c_i^\dagger t_{ij} c_j + h.c, \tag{1}$$

where the summation is over the nearest-neighbor bonds. The hopping matrix elements are given by $t_{j+\hat{x},j} = (-1)^{j_y}$ and $t_{j+\hat{y},j} = 1$, where $j = (j_x, j_y)$, $\hat{x} = (1, 0)$ and $\hat{y} = (0, 1)$. In the momentum space, the Hamiltonian is rewritten as

$$H_{pure} = 2 \sum_{(k_x,k_y)} \psi^\dagger_{(k_x,k_y)} \begin{pmatrix} \cos k_y & \cos k_x \\ \cos k_x & -\cos k_y \end{pmatrix} \psi_{(k_x,k_y)}, \tag{2}$$

where the summation is over the magnetic Brillouin zone $[-\pi, \pi) \times [0, \pi)$ and $\psi^\dagger_{(k_x,k_y)} = (c^\dagger_{(k_x,k_y)}, c^\dagger_{(k_x,k_y+\pi)})$. There are two energy bands $E(\mathbf{k}) = \pm 2\sqrt{\cos^2 k_x + \cos^2 k_y}$ on the magnetic Brillouin zone. They touch at two momenta, $\mathbf{k}^1 = (k^1_x, k^1_y) = (\pi/2, \pi/2)$ and $\mathbf{k}^2 = (k^2_x, k^2_y) = (-\pi/2, \pi/2)$. Near the degeneracies $\mathbf{k}^i$ $(i = 1, 2)$, they behave as $E(\mathbf{k}) \approx \pm 2\sqrt{(k_x - k^i_x)^2 + (k_y - k^i_y)^2}$ $(i = 1, 2)$. Define continuum variables $\Psi^\dagger(x, y) = (\psi_1{}^\dagger(x, y), \psi_2{}^\dagger(x, y), \psi_3{}^\dagger(x, y), \psi_4{}^\dagger(x, y))$ by $c_j \sim a[\, i^{j_x+j_y}\psi_1(x, y) + i^{j_x-j_y}\psi_2(x, y) +$

$i^{-j_x+j_y}\psi_3(x,y) + i^{-j_x-j_y}\psi_4(x,y)$], where a is the lattice spacing and $x = aj_x, y = aj_y$. Then the Hamiltonian becomes in the continuum limit ($a \to 0$)

$$\mathcal{H}_{pure} = 2i \int d\mathbf{x}\ \Psi^\dagger(x,y) \left[\begin{pmatrix} \sigma_1 & 0 \\ 0 & -\sigma_1 \end{pmatrix} \partial_x + \begin{pmatrix} \sigma_3 & 0 \\ 0 & \sigma_3 \end{pmatrix} \partial_y \right] \Psi(x,y). \tag{3}$$

Therefore our lattice model includes doubled massless Dirac fermions.

There are several subtleties for the massless Dirac fermions. When the Fermi energy lies at zero energy, that is, all the negative energy eigenstates are filled, the Hall conductivity σ_{xy} is ill defined. An infinitesimal mass determines the σ_{xy} in the continuum theory [13]. Similar phenomenon also occurs in a lattice model where an infinitesimal next-nearest-neighbor hopping t' opens a gap and the σ_{xy} is given by $t'/|t'|$ [3]. Therefore the massless Dirac fermions are at a quantum phase-transition point between differnt quantum Hall states.

Let us consider the effect of randomness in the hopping matrix elements. We set $t_{j+\hat{x},j} = (-)^{j_y} + \delta t_{j+\hat{x},j}$ and $t_{j+\hat{y},j} = 1 + \delta t_{j+\hat{y},j}$, where $\delta t_{j+\hat{x},j}$ and $\delta t_{j+\hat{y},j}$ are random variables and taken at random with constant probability from $[-W, W]$. It should be noted that this model preserves the time-reversal symmetry and belongs to the orthogonal ensemble. Another example of the orthogonal ensemble, Dirac fermions with diagonal disorder, was studied in [9,10] and it was suggested that all the eigenstates localize, which is consistent with the scaling theory of the Anderson localization [14]. In the case of the random-hopping model, however, it was found that the zero mode does not localize but become critical [8]. Similar phenomenon was found at the band center of the quantum Hall states [15]. In the quantum Hall states, however, the time-reversal symmetry is broken and the system belongs to a different universality class, the unitary ensemble. In [8], it was confirmed that parameters for the critical states form a critical line in the parameter space of the Hamiltonian, which is connected to pure massless Dirac fermions at zero energy. We consider that the stability of the zero modes against random hopping matrix elements is due to a symmetry of our Hamiltonian. The random hopping matrix elements preserves the symmetry in contrast to the diagonal disorder. In the language of the lattice Hamiltonian (1), the symmetry means that the transformation $c_j \to (-1)^{j_x+j_y} c_j$ induces sign change of the Hamiltonian.

Thus the eigenstates always appear in pairs with energies E and $-E$. The corresponding transformation in the continuum Hamiltonian (3) is given by $\mathcal{H}_{pure} \rightarrow \gamma^\dagger \mathcal{H}_{pure} \gamma = -\mathcal{H}_{pure}$, where $\gamma = \sigma_1 \otimes \sigma_1$. Since the random hopping matrix elements preserve the symmetry, the continuum Hamiltonian $\mathcal{H}$ for the random-hopping model also satisfies $\{\mathcal{H}, \gamma\} = \mathcal{H}\gamma + \gamma\mathcal{H} = 0$. Thus, taking the lowest order in derivatives, we obtain the following form as a possible Hamiltonian for the effective field theory

$$\mathcal{H} = 2i \int d\mathbf{x}\ \Psi^\dagger(x,y) \left[\begin{pmatrix} \sigma_1 & 0 \\ 0 & -\sigma_1 \end{pmatrix} \partial_x + \begin{pmatrix} \sigma_3 & 0 \\ 0 & \sigma_3 \end{pmatrix} \partial_y + \sum_{i=1}^{4} a_i(x,y)\ \gamma^i \right] \Psi(x,y), \tag{4}$$

where $\gamma^1 = \sigma_2 \otimes I$, $\gamma^2 = \sigma_1 \otimes \sigma_2$, $\gamma^3 = -\sigma_2 \otimes \sigma_1$, $\gamma^4 = I \otimes \sigma_2$ and $a_i(x,y)$ (i=1, $\cdots$, 4) are random variables.

In this paper, we study random Dirac fermions numerically beyond the zero modes. We diagonalize the Hamiltonian for finite squares of size $L^2 = 20^2$, 30^2, 40^2 and 50^2. To obtain reliable statistics, ensemble average over 16000, 16000, 8000 and 3360 realizations is performed respectively. The observables are density of states $\rho(E)$, the dimensionless conductance (Thouless number) $g(E)$ and the level-spacing distribution $P(s)$.

Let us first discuss the density of states $\rho(E) = 1/L^2 \sum_i \delta(E - E_i)$. When there is no randomness, the $\rho(E)$ vanishes linearly at zero energy. Recently, whether the density of states is finite or not at zero energy for random Dirac fermions is controversial [11,12]. The $\rho(E)$'s for different strength of the randomness are shown in Fig. 1. We have fitted the data by the power-law form $\rho(E) = CE^{\alpha(W)}$. Within the numerical accuracy, our results support the vanishing density of states at zero energy with an anomalous exponent $\alpha(W)$, which depends on strength of the randomness.

Next, in order to reveal nature of the eigenstates, let us consider the dimensionless conductance (Thouless number) $g(E)$. The $g(E)$ is defined by $g(E) = V(E)/\Delta(E)$, where $V(E)$ is an energy shift obtained by replacing periodic boundary condition by antiperiodic boundary condition and $\Delta(E)$ is a local mean level spacing near the energy E. Numerical results for the $g(E)$ are shown in Fig. 2 with L =30, 40 and 50, where ensemble average is performed within an energy window whose center is located at each data point. Rapid

enhancement of the $g(E)$ near zero energy is observed in Fig. 2. It suggests that the localization length grows rapidly near zero enrergy. This is consistent with the existence of crtitical states at zero energy. One may consider that the zero modes are just on the critical point. Then one of the possible scenarios is that the non-zero energy eigenstates are all off critical and therefore localized. It suggests an exponential dependence of the finite-size dimensionless conductance $g(E, L)$. The $g(E, L)$ obtained numerically decreases when the system size increases. It is, however, far from the exponential dependence. In Fig. 3, we have plotted the $g(E, L)$ as a function of $1/L$. It suggests a power-law form $g(E, L) \propto 1/L^{\gamma}$ rather than an exponential form $g(E, L) \propto \exp(-L/\xi)$. Although we can not exclude a possible existence of critical states in a finite energy region, we consider that the non-zero energy states may be localized in an infinite-size system and a crossover from the power-law form to an exponential form occurs when the system size increases beyond the localization length. The localization length of the eigenstates near zero energy may be large compared to the available system sizes and we may say that the power-law dependence of the $g(E, L)$ is a critical slowing down in the available finite-size system. This also suggests the existence of the critical state at zero energy.

We have also obtained the level-spacing distribution $P(s)$. The $P(s)$'s of the normalized energy separation $s = |E_n - E_{n+1}|/\Delta(E_n)$ are shown in Fig. 3 and 4, where E_n and E_{n+1} are two successive eigenenergies. The $P(s)$ is well described by the Wigner surmise $P(s) = As^{\beta}\exp(-Bs^2)$ in the metallic regime and becomes the Poissonian $P(s) = \exp(-s)$ in the insulating regime. The parameter β in the Wigner surmise reflects the symmetry of the Hamiltonian and β=1, 2 and 4 for the orthogonal ensemble, the unitary ensemble and the symplectic ensemble respectively. The parameters A and B are determined by $\int_0^{\infty} ds\ P(s) = 1$ and $\int_0^{\infty} ds\ sP(s) = 1$ and, in paticular, $A = \pi/2$ and $B = \pi/4$ for the orthogonal ensemble. The $P(s)$ characterizes nature of the eigenstates. States localized in different spatial regions are allowed to lie at the same energy. It means that the energy levels of the localized states distribute independently, which is described by the Poissonian. On the other hand, in metals where the eigenstates are extended, two adjacent energy levels

interact strongly, which brings strong energy repulsion and $P(s) \sim s^{\beta}$ near $s = 0$, where β is determined by the symmetry of the Hamiltonian. The $P(s)$ is well explained by a 2×2 random matrix model, which is the Wigner surmise. Level statistics near the mobilty edge has been studied recently and the appearance of critical level statistics is discussed [16]. Several numerical studies on level statistics near the mobility edge were performed for e.g. the three-dimensional Anderson model [18] and the band center of the quantum Hall states [19], which belong to the orthogonal ensemble and the unitary ensemble respectively, and it was found that the $P(s)$'s deviate from both the Wigner surmise and the Poissonian and exhibit critical behaviour, i.e., the $P(s)$'s do follow the Wigner surmise for small s and they then deviate from it at higher values of s and show stretched exponential decay. The $P(s)$'s near zero energy for our model are shown in Fig. 3, where the energy window is set $[0.1, 0.5]$ [20]. The location of the energy window is set sufficiently close to zero energy compared to the band width, which corresponds to the energy cut off in the continuum theory. Thus we consider that the system is described by random Dirac fermions. We confirmed that the $P(s)$'s near zero energy do not seriously depend on the system size and the location of the energy window. We consider that this is due to the fact that, since the location of the energy window is set near zero energy compared to strength of the randomness, the localization lengths are so long that it exceeds the system size. Thus, although the eigenstates may be localized in an infinite-size system, they behave as critical wavefunctions in a finite-size system. In fact, the $P(s)$ in Fig. 3 deviate from both the Wigner surmise and the Poissonian, and exhibit critical behaviour, i.e., the $P(s)$'s do follow the Wigner surmise for small s and they then deviate from it at higher values of s and show stretched exponential decay. On the other hand, when the location of energy window is set in other regions, non-critical behaviour is found (see Fig. 4). For example, when $L = 20$, $W = 0.5$ and the center of the energy window is set $E = 1.5$, the randomness is so weak that the deviation from pure massless Dirac fermion is small and the $P(s)$ is close to the Wigner surmise (see Fig. 4 (a)), and when $L = 50$, $W = 1.0$ and the center of the energy window is set $E = 3.75$, the localization length is within the system size and the Poissonian behaviour is observed (see

Fig. 4 (b)).

In summary, we have studied random Dirac fermions numerically beyond the zero modes. Although it belongs to the orthogonal ensemble, the zero-energy states do not localize and becomes critical. The density of states $\rho(E)$ vanishes as $\sim E^{\alpha}$ near zero energy and the exponent α depends on strength of the randomness W. It implies that scaling dimensions of the operators change with strength of the randomness. It is similar to the case of the random gauge-field critical line found in [7]. We consider that the existence of the symmetry $\{\mathcal{H}, \gamma\} = 0$ is crucial to have the criticality of the zero modes. We have studied nature of the eigenstates using the dimensionless conductance (Thouless number) $g(E)$ and the level spacing distribution $P(s)$. As is suggested by the numerical results for the $g(E)$, the localization length grows near zero energy so rapidly that it exceeds the available system size and the observables at non-zero energies exhibits anomalous behaviour, a critical slowing down. The $P(s)$'s near zero energy deviate from both the Wigner surmise and the Poissonian and exhibit critical behaviour, as in the case of the quantum Hall states, where rapid growth of the localization length and the critical behaviour of the $P(s)$ were observed [17,19]. We consider that it reflects the existence of critical states at zero energy for our model. As is discussed in [7], the random guage-field critical line is unstable in contrast to the critical line of (1+1)-dimensional free bosons, Tomonaga-Luttinger liquid, and a global renormalization-group flow for random Dirac fermions is not fully understood yet. Our results show that critical states can appear in a lattice model and we consider that our study gives a clue to understand a global phase diagram for random Dirac fermions on a lattice.

REFERENCES

[1] X. G. Wen and Y. S. Wu, *Phys. Rev. Lett.* **70**, 1501 (1993).

[2] W. Chen, M. P. A. Fisher and Y. S. Wu, *Phys. Rev. B* **48**, 13749 (1993).

[3] Y. Hatsugai and M. Kohmoto, *Phys. Rev. B* **42**, 8282 (1990).

[4] G. W. Semenoff, *Phys. Rev. Lett.* **53**, 2449 (1984).

[5] I. Affleck and J. B. Marston, *Phys. Rev. B* **37**, 3774 (1988).

[6] P. A. Lee, *Phys. Rev. Lett.* **71**, 1887 (1993).

[7] A. Ludwig, M. Fisher, R. Shankar and G. Grinstein, *Phys. Rev. B* **50**, 7526 (1994); C. Chamon, C Mudry and X. G. Wen, *Phys. Rev. B* **53**, 7638 (1996).

[8] Y. Hatsugai, X. G. Wen and M. Kohmoto, to be published in *Phys. Rev. B.*

[9] M. P. A. Fisher and E. Fradkin, *Nucl. Phys.* **B251**[FS13], 457 (1985).

[10] Y. Hatsugai and P. A. Lee, *Phys. Rev. B* **48**, 4204 (1993).

[11] A. A. Nersesyan, A. M. Tsvelik and F. Wegner, *Phys. Rev. Lett.* **72**, 2628 (1994).

[12] K. Ziegler, M. H. Hettler and P. J. Hirschfeld, *Phys. Rev. Lett.* **77**, 3013 (1996).

[13] S. Deser, R. Jackiw and S. Templeton, *Ann. Phys. (N.Y.)* **140**, 372 (1982); A. Niemi and G. W. Semenoff, *Phys. Rev. Lett.* **51**, 2077 (1983); N. Redlich, *Phys. Rev. D* **29**, 2366 (1984).

[14] E. Abrahams, P. W. Anderson, D. C. Licciardello and T. V. Ramakrishnan, *Phys. Rev. Lett.* **42**, 673 (1979).

[15] See, for a review, *The Quantum Hall Effect*, edited by R. E. Prange and S. M. Girvin (Springer, New York, 1990).

[16] V. E. Kratsov, I. V. Lerner, B. L. Altshuler and A. G. Aronov, *Phys. Rev. Lett.* **72**, 888

(1994).

[17] T. Ando, *J. Phys. Soc. Jpn* **52**, 1740 (1983); *J. Phys. Soc. Jpn* **53**, 3101 (1984); *J. Phys. Soc. Jpn* **53**, 3126 (1984).

[18] B. I. Shklovskii, B. Shapiro, B. R. Sears, P. Labrianides, and H. B. Shore, *Phys. Rev. B* **47**, 11487 (1993); S. N. Evangelou, *Phys. Rev. B* **49**, 16805 (1994).

[19] B. Huckstein and L. Schweitzer, *Phys. Rev. Lett.* **72**, 713 (1994); Y. Ono and T. Ohtsuki, *J. Phys. Soc. Jpn* **62**, 3813 (1993); Y. Avishai, Y. Hatsugai and M. Kohmoto, *Phys. Rev. B* **51**, 13419 (1995).

[20] We have also calculated $P(s)$'s for small energy windows near zero energy. We could not obtain systematic differences among them. Therefore we chose a rather wide energy window to obtain reliable statistics.

FIGURES

Fig. 1 The density of states $\rho(E)$, where $L = 50$ and $W = 0.7$, 0.8, 0.9 and 1.0. We have fitted the data by the power-law form $\rho(E) = CE^{\alpha(W)}$, where $\alpha(W) = 0.90$, 0.74, 0.55 and 0.39 for $W = 0.7$, 0.8, 0.9 and 1.0, respectively. We confirmed that the finite-size effect is small, comapring the results for $L = 50$ with those for $L = 30$ and 40.

Fig. 2 (a) The dimensionless conductance (Thouless number) $g(E)$, where $W = 1.0$ and $L = 30$, 40 and 50. (b) $1/L - g(E, L)$ plot for $E = 0.30$, 0.42, 0.50, 0.62 and 0.70. It suggests a power-law form $g(E, L) \propto 1/L^{\gamma}$ rather than an exponential form $g(E, L) \propto \exp(-L/\xi)$ in the present system size. We consider that it is a *critical slowing down* in the available finite-size system and a crossover from the power-law form to an exponential form occurs when the system size increases beyond the localization length.

Fig. 3 The level spacing distribution $P(s)$ near zero energy, where $L = 50$ and ensemble average is performed within an energy window $[0.1, 0.5]$. We confirmed that the finite-size effect is small, comapring the results for $L = 50$ with those for $L = 20$, 30 and 40. We also found that there is no substantial difference between results with energy windows $[0.1, 0.3]$, $[0.2, 0.4]$ and $[0.3, 0.5]$.

Fig. 4 The level spacing $P(s)$, (a) where $L = 20$, $W = 0.5$ and ensemble average is performed within an energy window $[2.0, 3.0]$; (b) where $L = 50$, $W = 1.0$ and ensemble average is performed within an energy window $[3.5, 4.0]$.

Fig. 1

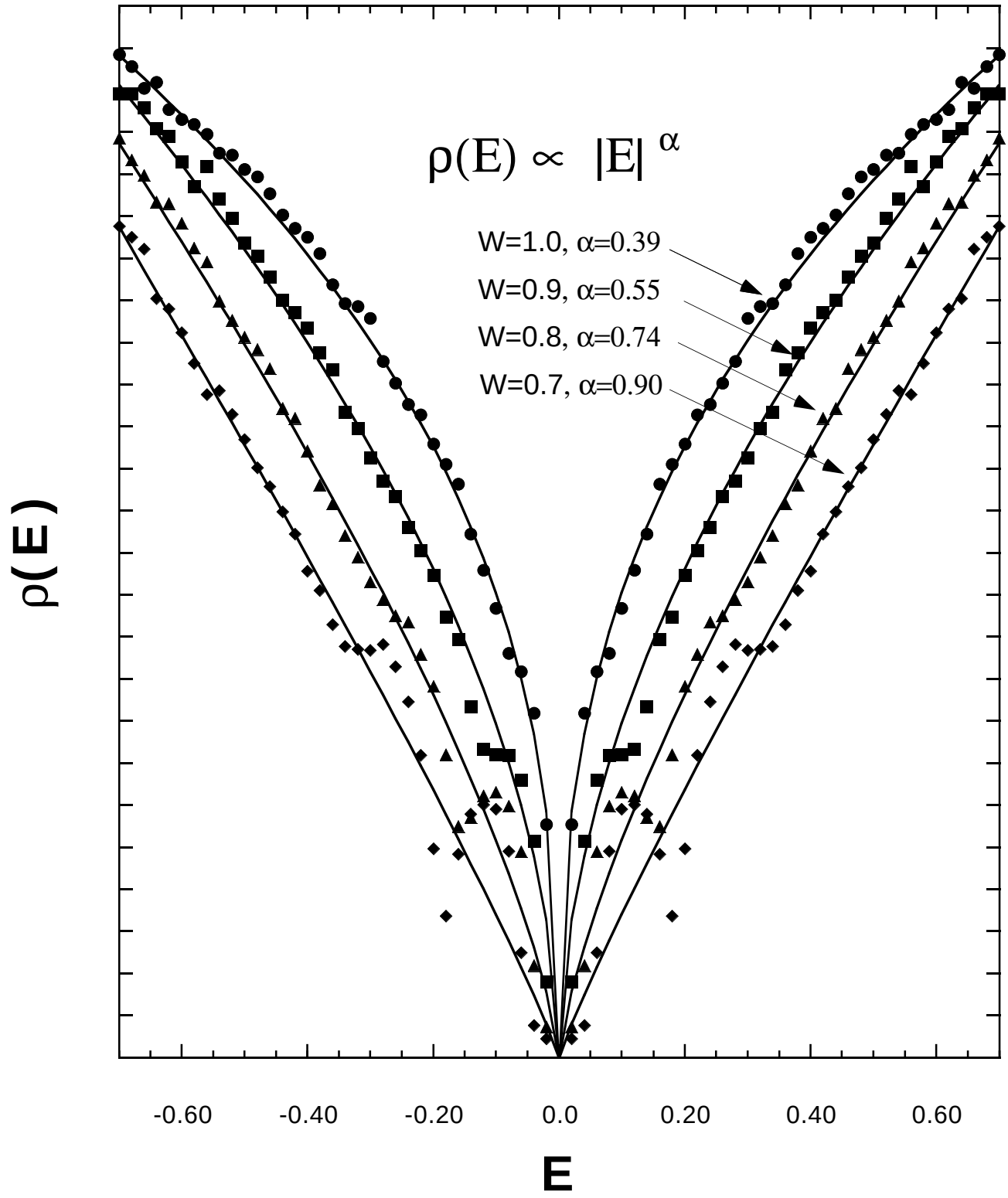
ρ(E) ∝ |E| α
W=1.0, α=0.39
W=0.9, α=0.55
W=0.8, α=0.74
W=0.7, α=0.90
ρ(E)
-0.60
-0.40
-0.20
0.0
0.20
0.40
0.60
E

Fig.2 (a)

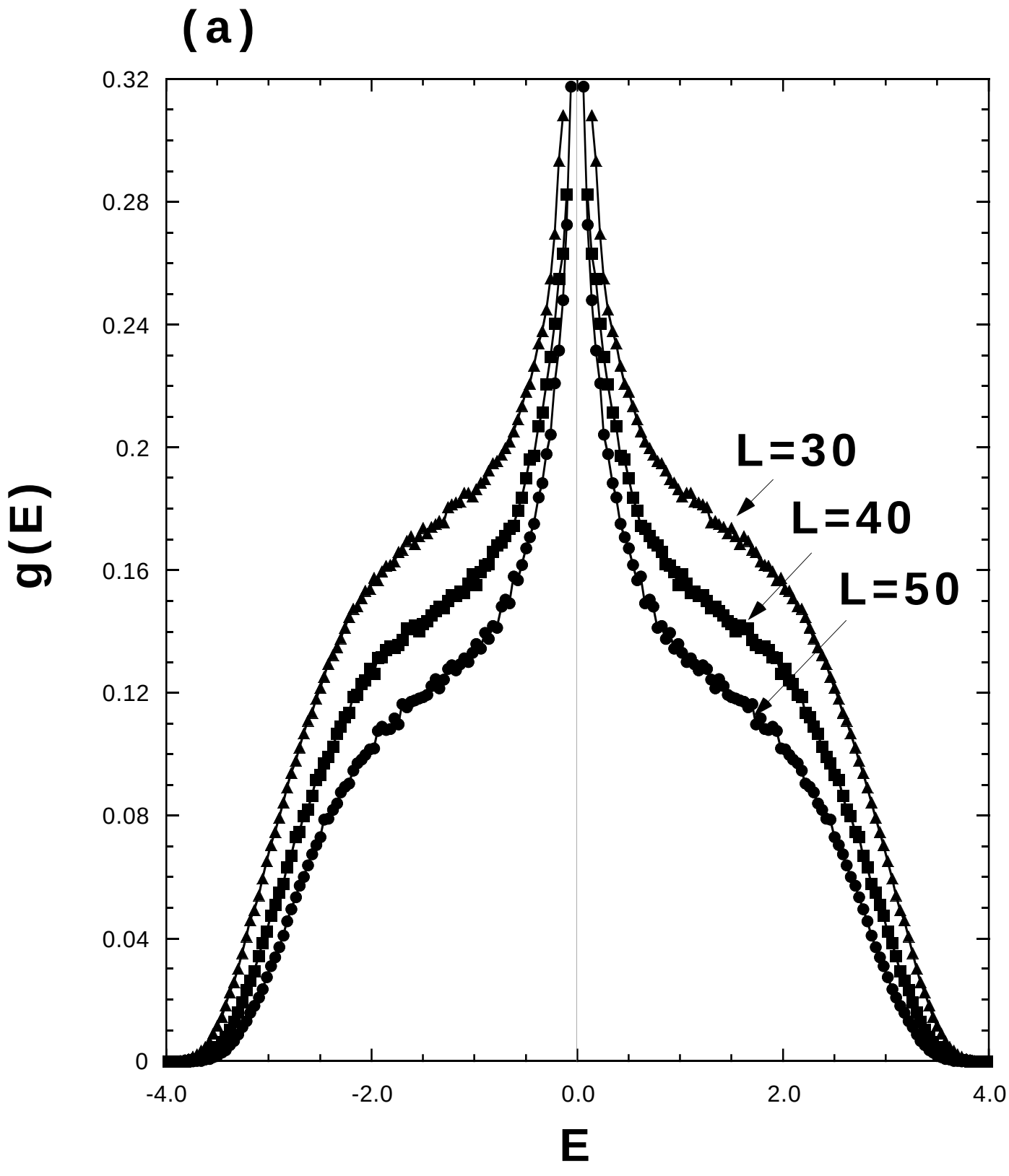

Fig.2 (b)

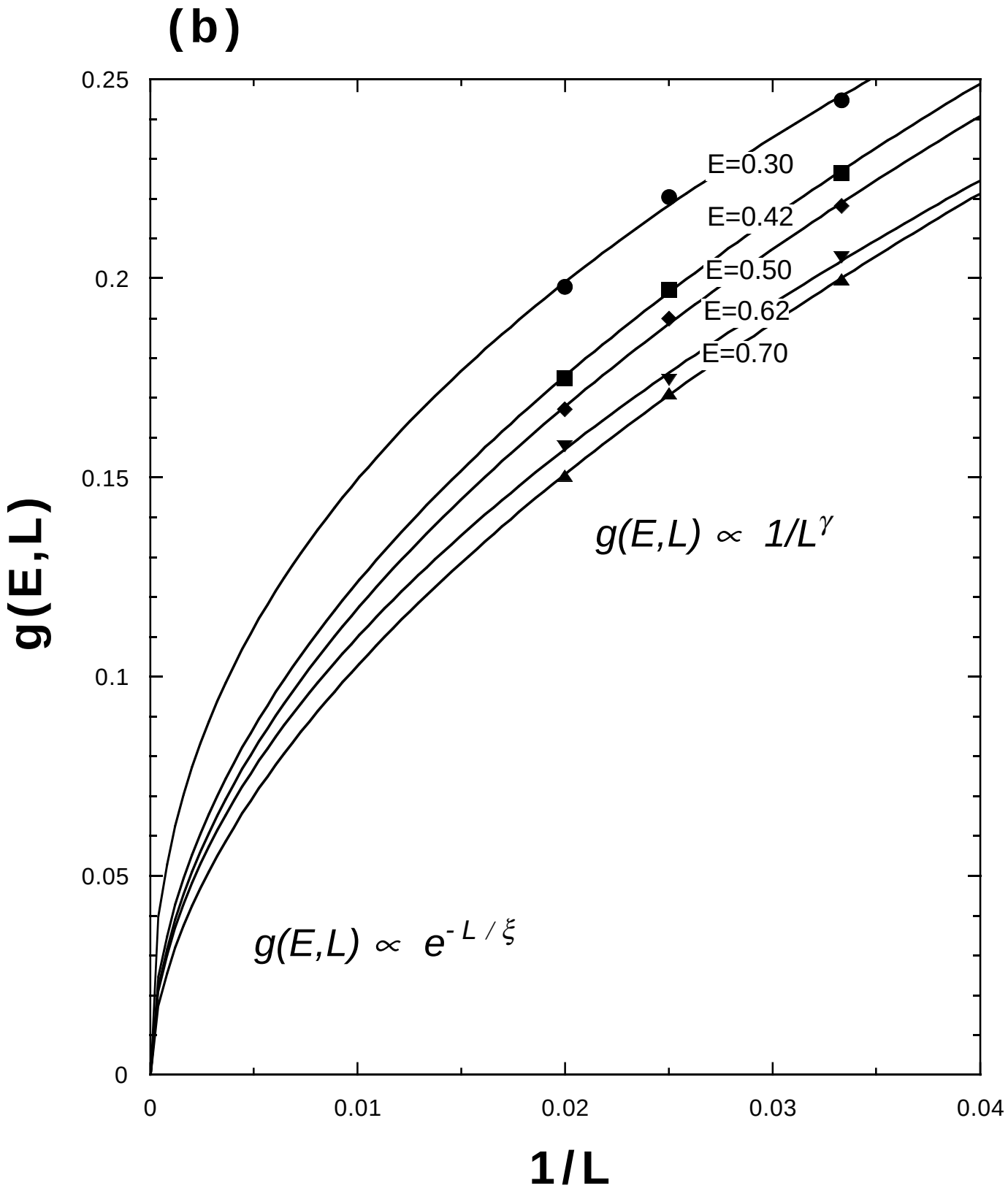
(b)
0.25
0.2
0.15
0.1
0.05
0
0
0.01
0.02
0.03
0.04
g(E,L)
1/L
E=0.30
E=0.42
E=0.50
E=0.62
E=0.70
g(E,L) ∝ 1/L^γ
g(E,L) ∝ e^-L/ξ

Fig. 3

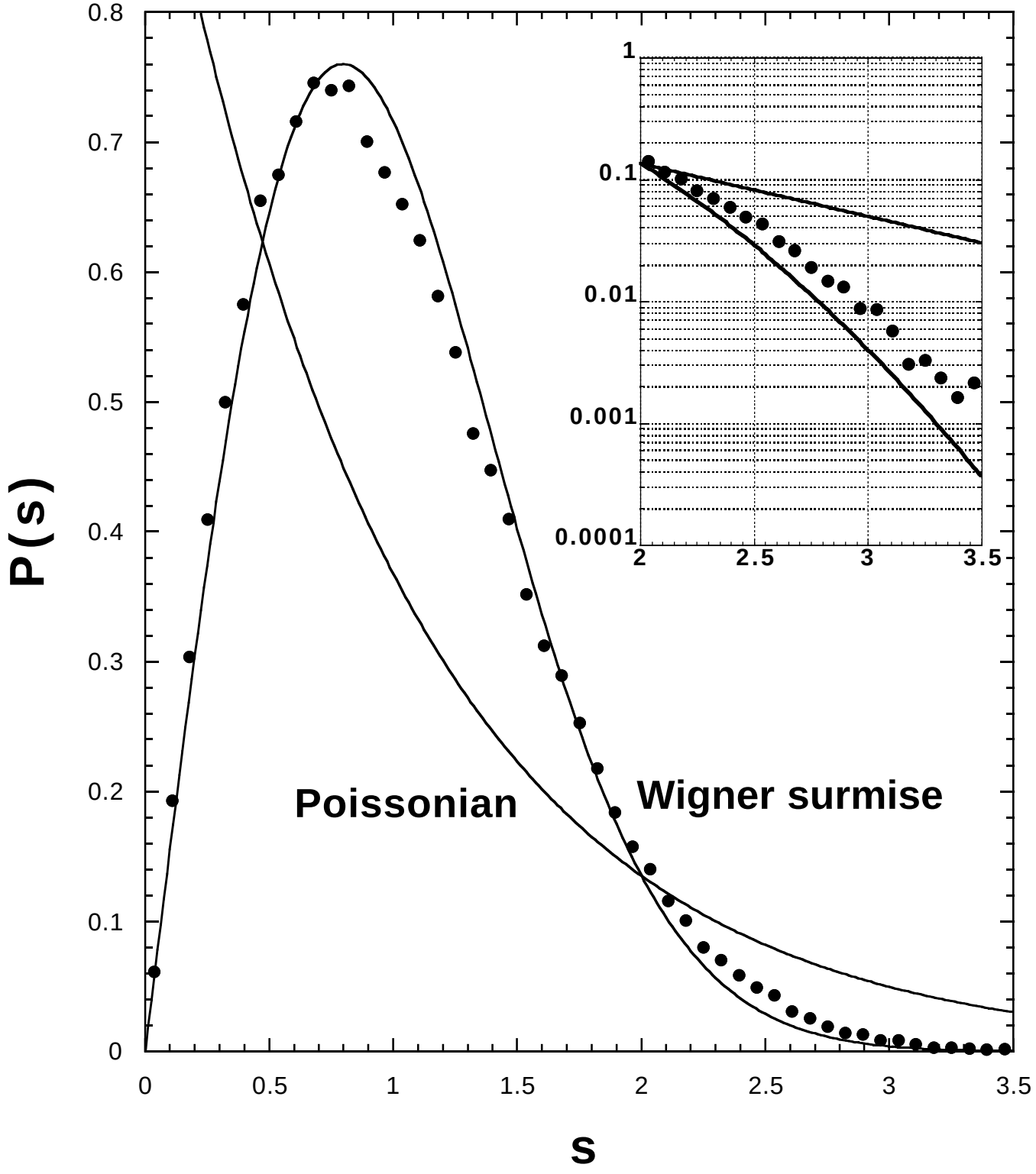
P(s)
s
Poissonian
Wigner surmise
0.8
0.7
0.6
0.5
0.4
0.3
0.2
0.1
0
0
0.5
1
1.5
2
2.5
3
3.5
1
0.1
0.01
0.001
0.0001
2
2.5
3
3.5

Fig. 4 (a)

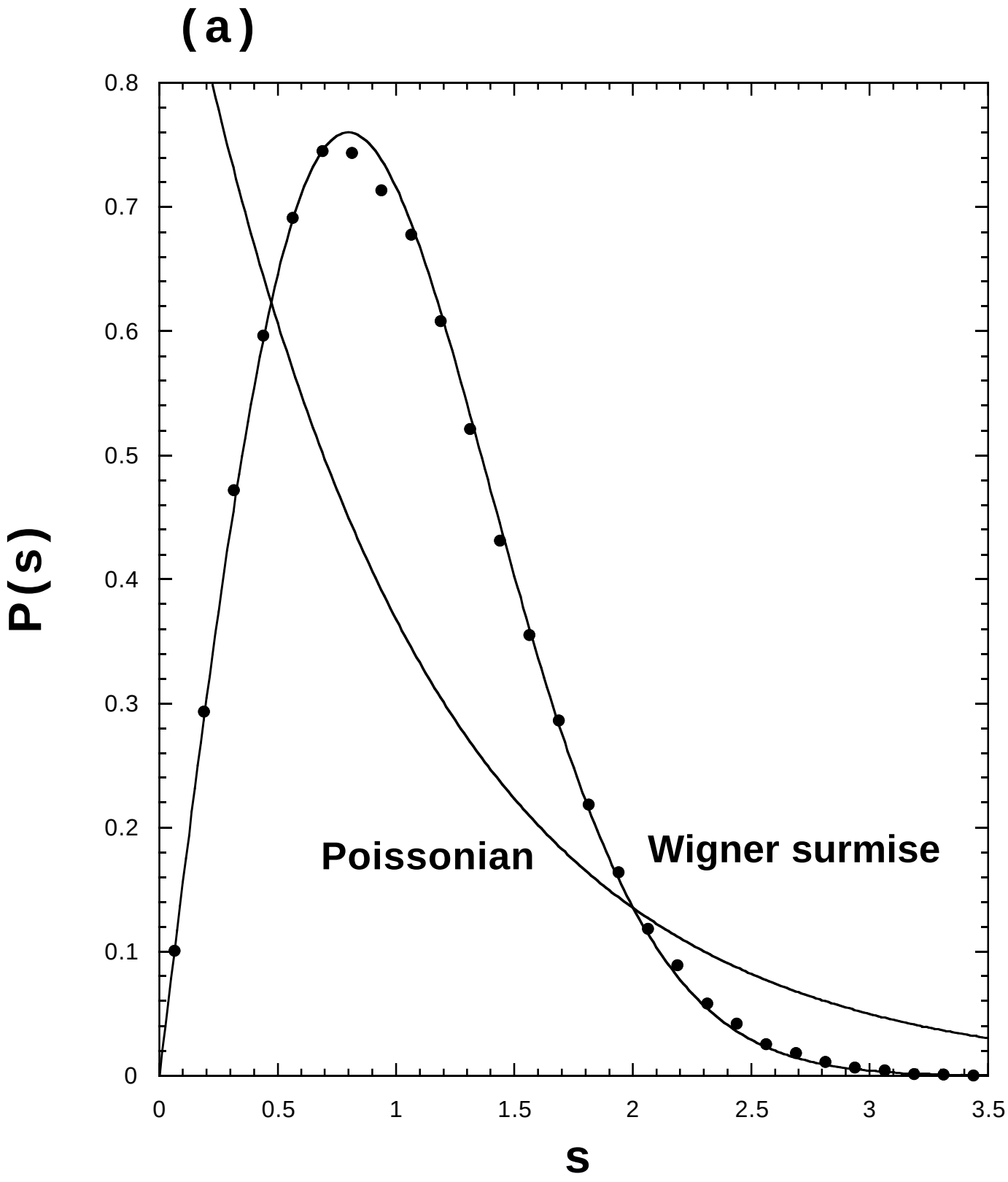
(a)
P(s)
s
Poissonian
Wigner surmise
0
0.1
0.2
0.3
0.4
0.5
0.6
0.7
0.8
0
0.5
1
1.5
2
2.5
3
3.5

Fig. 4 (b)

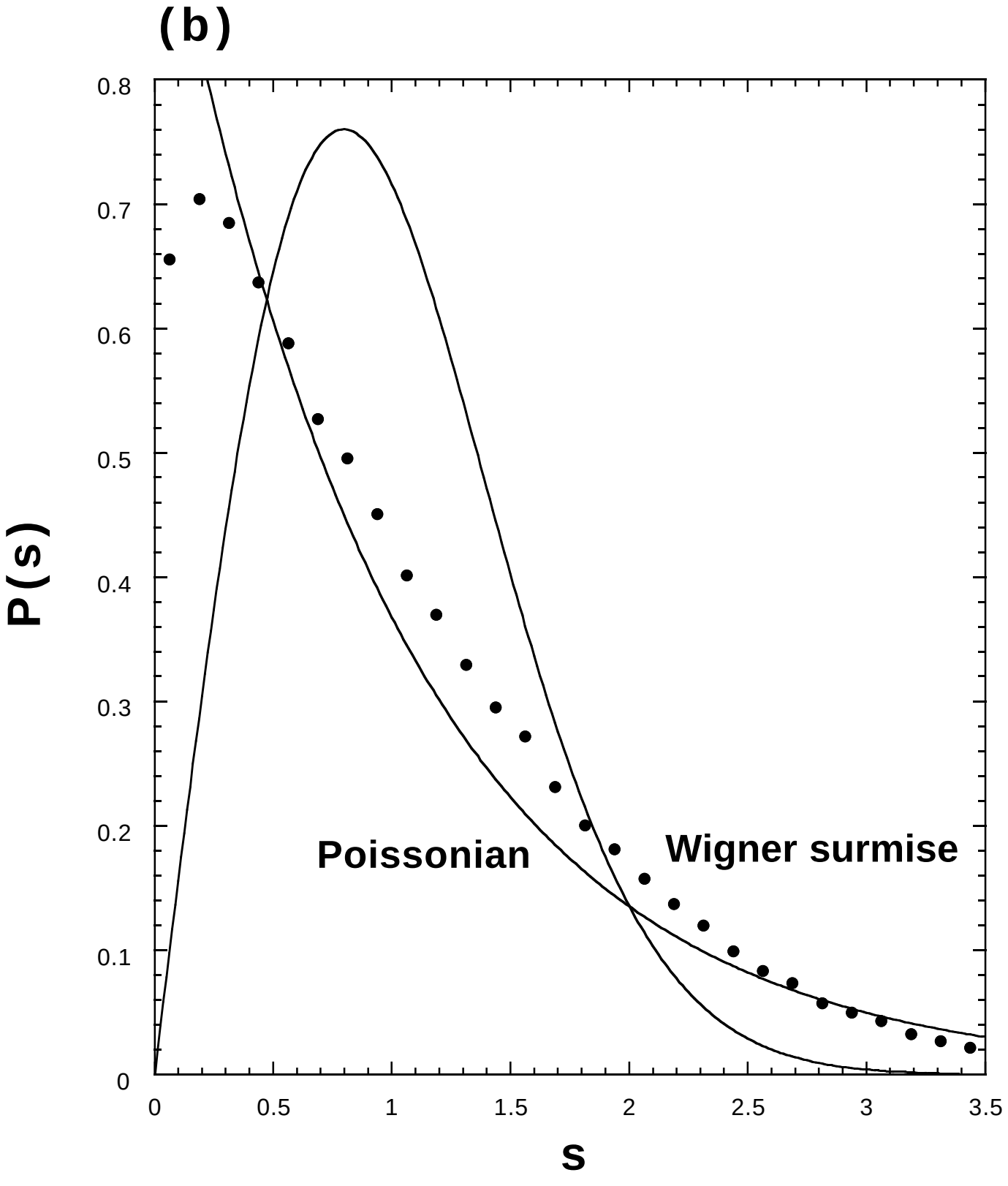
(b)
P(s)
s
Poissonian
Wigner surmise
0
0.1
0.2
0.3
0.4
0.5
0.6
0.7
0.8
0
0.5
1
1.5
2
2.5
3
3.5